

Dynamics of Optical Limiting in Heavy-Atom Substituted Phthalocyanines

Kamjou Mansour,[†] Daniel Alvarez, Jr.,[§] Kelly J. Perry,[†] Ingrid Choong,[§]
Seth R. Marder,^{†§} and Joseph W. Perry[†]

[†]) Jet Propulsion Laboratory
California Institute of Technology
Pasadena, CA 91109

[§]) Beckman Institute
California Institute of Technology
Pasadena, CA 91125

ABSTRACT

Picosecond and nanosecond nonlinear transmission measurements were used to determine the excited singlet- and triplet-state absorption cross sections at 532 nm for group IVA metalloid phthalocyanines. A five-state rate-equation model is used to analyze the nonlinear transmission data. The successful simulations of the nonlinear transmission data on Ibis series of phthalocyanines for widely differing pulse durations provide strong evidence for the validity of the excited state absorption model. Use of the heavy atom effect has allowed engineering of phthalocyanines with strongly enhanced optical limiting performance.

1. INTRODUCTION

Materials that exhibit nonlinear absorption are currently of interest for use in devices that protect sensors and eyes from energetic light pulses, as well as for other optical limiting or switching applications. Optical limiting has been reported for various organic dyes and complexes such as tetraphenylporphyrins,¹ indanthrone derivatives and oligomers,² metallophthalocyanines,³ iron-cobalt metal clusters,⁴ metallonaphthalocyanines⁵ and C₆₀ (Buckminsterfullerene).⁶ Optical limiting in these organic dyes has been attributed to nonlinear absorption, where the absorption induced at the excitation wavelength is stronger than the initial small-signal absorption by the ground state. Such nonlinear absorbers have been referred to as reverse saturable absorbers (RSA) or excited-state absorbers. In general, the effectiveness of RSA molecules for optical limiting applications is mainly determined by the ratio of the excited-state absorption strength to that of the ground state in the relevant spectral region.

Previously, optical limiting in metallophthalocyanines such as chloroaluminum phthalocyanine (CAP) and bis(tri-*n*-hexylsiloxy) silicon naphthalocyanine (SiNc) for picosecond and nanosecond laser pulses was investigated.^{5,7} These studies suggested the importance of excited singlet-singlet and triplet-triplet absorption to the optical limiting for different time regimes. Wic et al.⁷ reported the excited singlet-singlet absorption cross-sections (σ_s). The ratio of excited-state to ground-state absorption cross sections (σ_s/σ_g) at 532 nm for CAP and SiNc were 10.5 and 14, respectively, for 30-60 picosecond pulses. Nanosecond transient absorption measurements on CAP⁸ and SiNc⁹ indicate that substantially larger absorption cross-sections on the order of 30-50 times that of the ground-state absorption cross-section are exhibited by the triplet-triplet absorption, but these are offset by relatively small triplet yields. This led us to use the heavy atom effect as an approach to enhancing the nonlinear absorption of phthalocyanines. Increasing the atomic number of the central atom increases the effective spin-orbit coupling for the π -electrons and, therefore, the intersystem crossing rate from singlet to triplet states. With efficient population of the triplet state, one would expect to enhance the nonlinear absorption in these molecules for laser pulse durations shorter than the lifetime of the triplet states (typically less than 400 μ sec).

We have recently demonstrated¹⁰ for a series of phthalocyanines containing metalloid atoms (silicon, germanium and tin) that the heavier atoms lead to enhanced optical limiting for nanosecond laser pulses. Evidence for triplet-state enhancement of the optical limiting was obtained from measurements with different pulse widths, i.e. 8 ns as compared to 70 ps, 532 nm laser pulses. We observed that the nonlinear absorption increases in the order of SiPc, GePc and SnPc for nanosecond pulses, but the picosecond nonlinear absorption, due only to excited singlet state absorption, follows the opposite trend. Thus, on a timescale where the excited singlet state is decaying and the triplet state population is increasing, molecules with heavier metalloid atoms exhibit enhanced nonlinear absorption. This strategy has indeed led to engineering of phthalocyanine dyes with enhanced optical limiting response. For example, the strong-signal optical limiting output of SnPc is a factor of six lower than CAP and a factor of two lower than SiNc, for solutions with 67% linear transmission in an $f/\#$ 19.7 optical limiting geometry,

In this paper, we present an analysis of the nonlinear transmission of the group IVA metalloid phthalocyanines that determines their excited-state absorption cross sections at 532 nm. The structures of these compounds, prepared using literature methods,¹¹⁻¹⁴ are shown in Figure 1. A five-state rate-equation model provides a good description of the nonlinear transmission on picosecond and nanosecond timescales over a wide range of pulse energies. Triplet-triplet absorption spectra in the visible are presented.

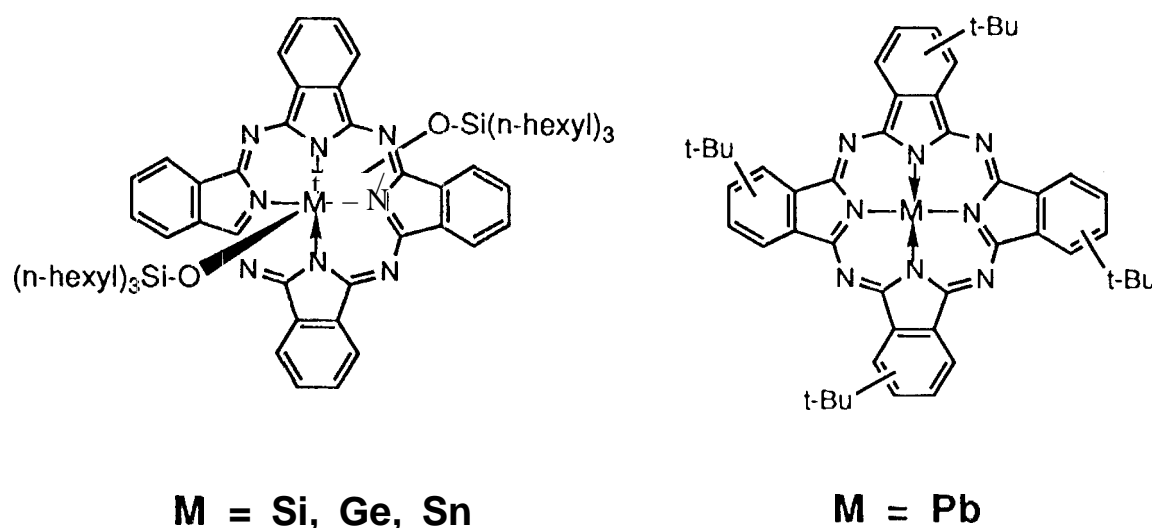


Figure 1. Molecular structures of soluble group IVA metalloid substituted phthalocyanines.

2. KINETICS OF EXCITED-STATE ABSORPTION

A state diagram relevant to excited-state absorption in organic dyes is shown in Figure 2. Metallophthalocyanines exhibit strong electronic transitions in the visible (Q band at ~700 nm) and in the near UV (B or Soret band at 300-400 nm). Both the Q [$1a_{1u}(\pi) \rightarrow 1e_g(\pi^*)$] and B [$1a_{2u}(\pi) + 1e_g(\pi^*)$] bands arise from transitions to π - π^* states of E_u symmetry.¹⁵ For optical wavelengths between the B and Q bands (400-600 nm) excitation will be to high vibrational levels of the first excited singlet state, S_1 , or to weakly allowed electronic states, and fast relaxation to the lower vibrational levels of S_1 occurs. Subsequent excited-state singlet-singlet transitions can occur and may involve promotion of an electron from the $1e_g$ orbital to $1b_{1u}$ or $1b_{2u}$ orbitals. The upper excited singlet states typically have ultrafast relaxation to S_1 with a time constant on the order of one picosecond. Intersystem crossing from S_1 competes with fluorescence and internal conversion, giving rise to population of the lowest triplet state and triplet-triplet absorption.

The transmission of a system described by the state diagram in Figure 2 will depend, assuming fast dephasing, on the populations of the ground and excited states, as well as the various absorption cross-sections. ^{1,7,9-20} The rate equations describing the electronic state populations for the five-state model are:

$$\frac{dN_0}{dt} = -\sigma_{01} N_0 \Phi + k_{10} N_1 + k_{30} N_3 \quad (1)$$

$$\frac{dN_1}{dt} = \sigma_{01} N_0 \Phi - \sigma_{12} N_1 \Phi - (k_{10} + k_{13}) N_1 + k_{21} N_2 \quad (2)$$

$$\frac{dN_2}{dt} = \sigma_{12} N_1 \Phi - k_{21} N_2 \quad (3)$$

$$\frac{dN_3}{dt} = -\sigma_{34} N_3 \Phi - k_{30} N_3 + k_{13} N_1 \quad (4)$$

$$\frac{dN_4}{dt} = \sigma_{34} N_3 \Phi - k_{43} N_4 \quad (5)$$

subject to $N_0(0) = N_0(t) + N_1(t) + N_2(t) + N_3(t) + N_4(t)$ and $N_1(0), N_2(0), N_3(0)$, and $N_4(0) = 0$, where N is the number density of the subscripted state ($S_0 \equiv 0, S_1 \equiv 1, S_2 \equiv 2, T_1 \equiv 3$ and $T_n \equiv 4$), Φ is the photon flux (i.e. $I/h\nu$) in photons/cm²sec, and σ and k are the absorption cross section and spontaneous decay rate between subscripted states, respectively. The propagation equation for an optical pulse is, assuming a slowly varying envelope approximation:

$$\frac{d\Phi}{dz} = -\sigma_{01} N_0 \Phi - \sigma_{12} N_1 \Phi - \sigma_{34} N_3 \Phi. \quad (6)$$

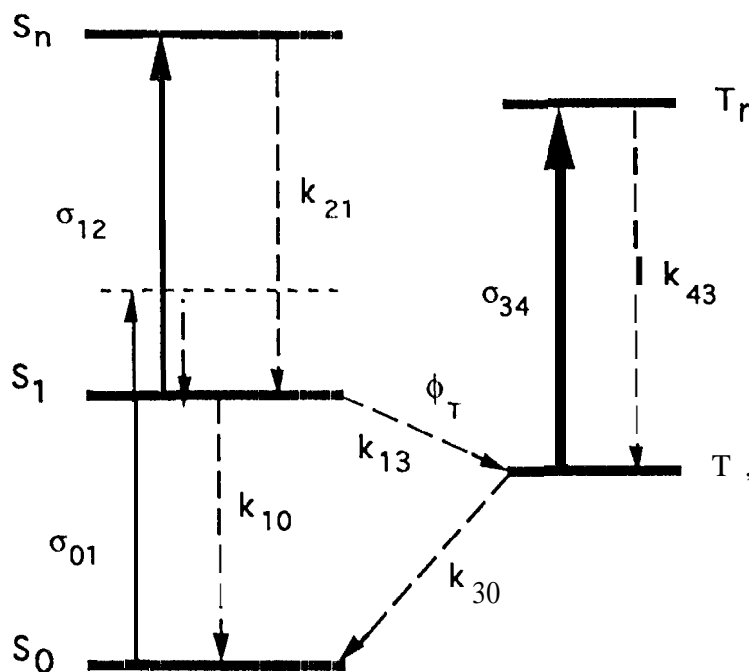


Figure 2. Five-state model for nonlinear absorption behavior of metallophthalocyanines. Symbols are defined in the text.

With a specification of the material parameters: $N_0(0)$, the σ values, the various photophysical rate constants and pathlength, l , and the optical pulse characteristics: pulse energy, duration, shape in time and transverse profile, the equations can be solved to give the transmission. A Fortran program was developed to numerically solve the coupled rate equations for the time integrated transmission of optical pulses. Input pulse profiles were taken as Gaussian functions in time and space and the transmission was averaged over the transverse profile. The excited state absorption cross-sections, σ_{12} and σ_{34} , were adjusted to give a best fit to the experimental transmission versus pulse energy data, with other parameters determined separately and held fixed in value. In the next section, the photophysical parameters for the phthalocyanines will be specified and determination of the excited state absorption cross-sections by fitting the nonlinear transmission data will be discussed.

3. EXCITED-STATE ABSORPTION CROSS SECTIONS OF GROUP IVA METALLOPHthalOCYANINES

3.1. Photophysical properties

To extract the absorption cross sections for the singlet-singlet, σ_{12} , and triplet-triplet, σ_{34} , transitions from nonlinear transmission data using the rate-equation model described earlier, the values of the excited-state decay rates k_{10} , k_{21} , k_{13} , k_{43} , k_{30} and the ground-state absorption cross section, σ_{01} , must be known. Table 1 summarizes the peak wavelength of the Q-band absorption, λ_{\max} , the S_1 fluorescence lifetime, $\tau_S = 1/(k_{10} + k_{13})$, and the triplet yield, $\Phi_T = k_{13}/(k_{10} + k_{13})$, for the group IVA metalloid phthalocyanines and SiNc. The fluorescence lifetimes were directly determined using time-correlated single-photon counting. Direct experimental Φ_T values for the phthalocyanines are not yet available, but were roughly estimated from experimental fluorescence yields and an estimate of the internal conversion yield Φ_{ic} . Φ_{ic} for SiNc was determined from a measurement of Φ_f and the known Φ_T , using $\Phi_{ic} = 1 - \Phi_T - \Phi_f$. Φ_f was determined for SiNc and the phthalocyanines in toluene solutions, using a relative method. For SiNc $\Phi_f = 0.45$ and, therefore, $\Phi_{ic} = 0.35$. Taking Φ_{ic} for the group IVA metalloid phthalocyanines to be the same as for SiNc allowed the rough estimates of Φ_T in Table 1 to be made. The shortening of the S_1 lifetime and the increase in the triplet yields of the phthalocyanines upon heavy atom substitution is evident. The radiative lifetimes of these molecules, calculated using a Strickler-Berg analysis,²¹ agreed to within 10% of those obtained using $k_{rad} = \Phi_f / \tau_S$. The upper excited-state non-radiative relaxation rates, k_{21} and k_{43} , were assumed to be 1 ps. The decay of the first triplet state, T_1 , to the ground state occurs on a much slower time scale than k_{13} . For example, k_{13} for SiNc was reported⁹ to be $(330 \mu s)^{-1}$ in deaerated solutions. The triplet relaxation in aerated solutions is biexponential with decay times of ~ 2 and $42 \mu s$.⁹ In all cases, the T_1 decay time is much longer than the pulse durations used in this study. The ground-state absorption cross sections, σ_{01} , are determined from linear absorption measurements and are listed in Table 2.

TABLE 1. Photophysical parameters of group IVA metal substituted phthalocyanines

Molecule	λ_{\max} (nm)	τ_S (ns)	Φ_T
SiNc ^a	774	$3.15 \pm 0.05^{(5)}$	$0.20 \pm 0.03^{(9)}$
SiPc ^b	664	4.5 ± 0.10	0.35 ^d
GePc ^b	667	4.2 ± 0.10	0.37 ^d
SnPc ^b	678	2.0 ± 0.10	0.55 ^d
PbPc ^c	714	0.7 ± 0.10	0.70 ^d

—a) Molecule of the form: $M(OSi(C_6H_{13})_3)_2Nc$

b) Molecule of the form: $M(OSi(C_6H_{13})_3)_2Pc$

c) Molecule of the form: $MPc(t-C_4H_9)_4$

d) Estimated values, refer to text. Precision estimated to be $\pm 20\%$

3.2. Analysis of picosecond and nanosecond nonlinear transmission

3.2.1. Experiment

A single beam experimental arrangement was used to measure the nanosecond nonlinear transmission. The excitation source was a frequency-doubled Q-switched Nd:YAG laser (Quantel 660) modified to operate in a TEM₀₀ transverse mode with an 8 ns (FWHM) multimode pulse envelope. The laser pulses were focussed into 1-cm pathlength solutions by a 50-cm "best form" lens that provided a Gaussian spatial intensity profile of 135 μm radius (I_{1/e^2}). The Rayleigh range was about 11 cm giving rise to essentially collimated beam propagation through the 1-cm cuvettes. The transmitted pulse was detected with a silicon photodiode of 1 cm^2 active area placed 15 cm behind the sample. The detector was placed close to the sample in order to collect all the transmitted energy. Thus, changes in the transmitted energy for incident energies up to the breakdown threshold are due only to absorption processes in the solutions. The incident pulse energy was monitored on every shot by using a beam splitter to direct a fraction of the incident beam to another photodiode. The photodiodes were calibrated with a Scientech model 362 power meter. A series combination of polarizers and half-wave plates were used as variable attenuators for energy-dependent measurements.

A similar optical arrangement was utilized for picosecond nonlinear transmission measurements. The picosecond pulses were produced by injection of continuous-wave mode-locked Nd:YAG output into a 10-Hz Nd:YAG regenerative amplifier, followed by frequency doubling. The laser operated in a near Gaussian profile and produced temporally Gaussian pulses of nominally 70 ps (FWHM) duration. The laser pulses were focused into the sample, again using 50 cm "best form" lens, to provide a roughly Gaussian spatial intensity profile of 61 μm (I_{1/e^2}). The rest of the geometry was the same as for the nanosecond measurements.

3.2.2. Results

Figures 3 and 4 show nonlinear transmission curves for SiPC and SnPC solutions for picosecond and nanosecond pulses, respectively. Experimental nonlinear transmission data have been obtained for pulse energies spanning over more than three orders of magnitude. The data are shown along with best fit theoretical simulations calculated using the five-state rate-equation model. At low incident energies the transmission approaches the linear transmission of the solutions. With increasing pulse energy the transmission drops and ultimately begins to approach a limit for the highest energy range. The results in Figures 3 and 4 were obtained for dye concentrations of about 2.0×10^{-4} M. Additional measurements of nanosecond and picosecond nonlinear transmission of SiNc, SiPC, GcPC, SnPC and PbPC in toluene solutions were performed for concentrations varying from 8×10^{-5} to 5.5×10^{-4} M.

3.2.3. Rate equation analysis and excited-state absorption cross sections

The rate-equation model described earlier involving excited singlet and triplet states was implemented to fit the nonlinear transmission responses of the various phthalocyanines. The fitting strategy followed to extract the excited-state absorption cross sections was to first fit the 70 ps picosecond data for each molecule, these data being dominated by the excited-singlet absorption, thus establishing the excited-singlet absorption cross sections. We then fit the 8 ns nonlinear transmission data, holding the excited-singlet absorption cross sections fixed, to obtain the triplet-triplet absorption cross sections.

Figure 3 shows the best theoretical fits for SiPC and SnPC solutions for 70 ps pulses. The photophysical parameters needed for generating the numerical fits for each molecule were described in section 3.1. The numerical fits are in good agreement with the data for incident energies up to about 100 μJ at which point the theoretical transmission reaches a minimum and begins to increase, departing from the experimental data. This calculated behavior is due to saturation of population in the upper excited singlet state and will be discussed below. Analysis of the data for the various phthalocyanines leads to the values for σ_{12} listed in Table 2. The σ_{12} value obtained for SiNc is in agreement with the value previously reported⁷.

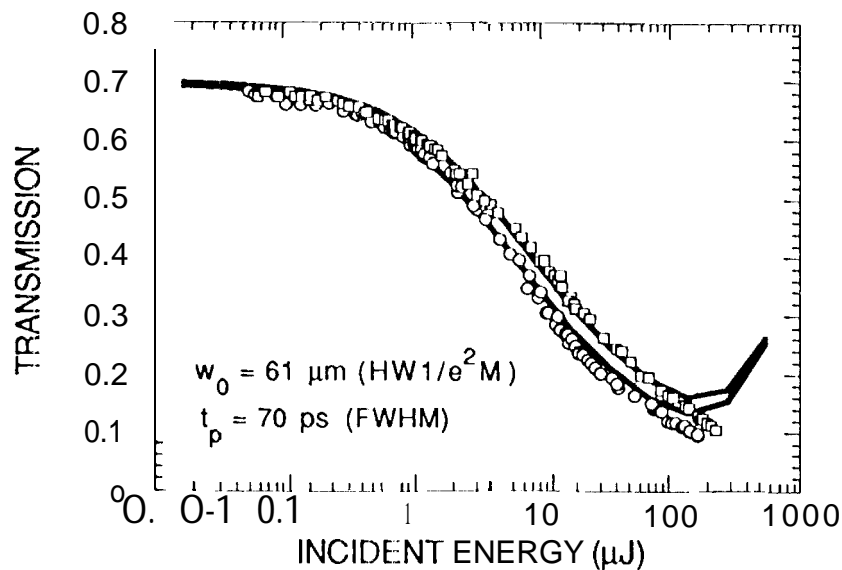


Figure 3. Nonlinear transmission of SiPc (circles) and SnPc (squares) dyes in toluene solution for 70 psec, 532 nm laser pulses. Solutions had 70% linear transmission at 532 nm for 1 cm pathlength. Solid curves are the best theoretical fits to the five-state rate-equation model.

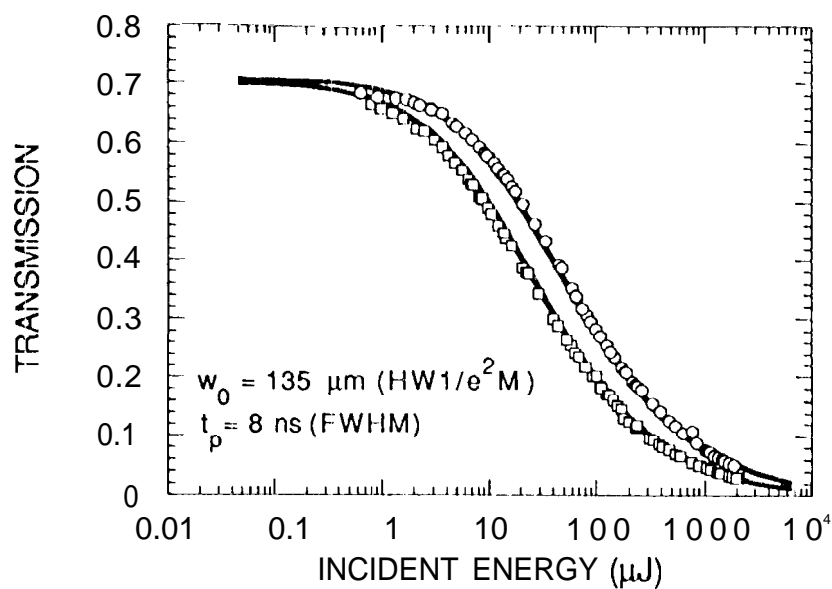


Figure 4. Nonlinear transmission of SiPc (circles) and SnPc (squares) dyes in toluene solution for 8 ns, 532 nm laser pulses. Solutions had 70% linear transmission at 532 nm for 1 cm pathlength. Solid curves are the best theoretical fits to five-state rate-equation model.

in figure 4, the best theoretical fits for SiPc and SnPC for 8 ns pulses are shown. Using σ_{12} obtained from the analysis of the picosecond data, along with the other photophysical parameters, as fixed parameters, numerical fits of the 8 ns nonlinear transmission data allowed σ_{34} to be established. The rate-equation model successfully simulates the nanosecond nonlinear transmissions for this series of phthalocyanines over the full range of incident pulse energies. The extracted values for σ_{34} are listed in Table 2. The σ_{34} value obtained for SiNc agrees with the extinction coefficient of the triplet-triplet transient absorption reported by Firey *et al.*⁹ Excellent simulations of the experimental nonlinear transmission were obtained for solutions with varying dye concentrations, using a single set of parameters.

In the calculated picosecond nonlinear transmission we observe a strong bleaching effect for pulse energies above 100 μJ . This behavior is due to kinetic saturation of population in the upper excited singlet state. In the limit where the intensity is high enough that the pumping rate, 6120 , competes with the decay rate k_{21} , assumed earlier to be $(1 \text{ ps})^{-1}$, population will build up in S_n . Since no additional absorption from this state is included in the model, the calculated transmission will rise and approach unity as the S_n population saturates. If k_{21} used in the calculation is increased the bleaching effect is reduced, however for low concentration solutions, the high energy behavior deviates from the experimental data even for rates as high as $(1 \text{ O fs})^{-1}$. This suggests that additional loss channels, such as absorption from S_n to even higher singlet states or nonlinear refractive beam spreading, not accounted for in the model are affecting the measured transmission. Nonetheless, σ_{12} is well defined by the lower energy ($<100 \mu\text{J}$) data, particularly for higher concentrations.

TABLE 2 Absorption Cross Sections^a for Group IVA Metalloid Phthalocyanines

Molecule	σ_{01}	σ_{12}	σ_{12}/σ_{01}	σ_{34}	σ_{34}/σ_{01}	$\phi_T \sigma_{34}/\sigma_{01}$
SiNc ^b	2.8	39	14	90	32	6.4
SiPc ^c	2.4	30	13	48	20	7.0
GcPc ^c	2.3	30	13	51	22	8.2
SnPc ^c	2.1	22	11	67	32	18
PbPc ^d	1.4	42	30	33	23	16

- a) Cross sections given in units of 10^{18} cm^2 . Estimated precision in cross sections: $\sigma_{01}(\pm 5\%)$, σ_{12} ($\pm 10\%$) and $\sigma_{34}(\pm 20\%)$.
b) Molecule of the form: $\text{Si}(\text{OSi}(\text{C}_6\text{H}_{13})_3)_2\text{Nc}$.
c) Molecule of the form: $\text{M}(\text{OSi}(\text{C}_6\text{H}_{13})_3)_2\text{Pc}$.
d) Molecule of the form: $\text{MPc}(\text{t-C}_4\text{H}_9)_4$.

The values of σ_{01} and σ_{12} show a slight decrease in going from SiPc to GcPc to SnPc, leading to a nearly constant ratio, $R_S = \sigma_{12} / \sigma_{01}$. However, for PbPc σ_{01} is yet smaller and σ_{12} is larger than for SnPc, leading to a substantially larger R_S than for the other phthalocyanines. Indeed, PbPc shows a lower strong-signal picosecond nonlinear transmission than the other molecules. The values of σ_{34} for the phthalocyanines determined by fitting the nanosecond transmission data are dependent on the estimated values for ϕ_T , thus their accuracy is limited by the uncertainty in the estimates. However, the product $\phi_T \sigma_{34}$ is well determined by the analysis, so we have also listed in Table 2 the ratio $R_T = \phi_T \sigma_{34} / \sigma_{01}$. The σ_{34} values for SiPc, GcPc and SnPc comparable and the value for PbPc is somewhat reduced, but the $\sigma_{34} / \sigma_{01}$ ratios are roughly constant. It is not known whether the differences in the parameters for PbPc and the other phthalocyanines are due to the metal or the different ring substitution, i.e. tetra-*t*-butyl for the PbPc versus unsubstituted for the other molecules. The values of R_T for the phthalocyanines show that heavy atom substitution leads to an enhanced triplet-triplet contribution to the nanosecond nonlinear transmission in these molecules.

With values for the excited-state cross sections and the photophysical parameters, i.e. τ_S and ϕ_T , an assessment of the relative contributions of excited singlet-singlet and triplet-triplet absorption to the optical limiting of the

phthalocyanines for various pulse durations can be made. As discussed above, for pulse durations much less than τ_S the optical limiting response is dominated by singlet-singlet absorption. When pulse durations are much larger than τ_S the singlet contribution diminishes and the contribution of the triplet-triplet absorption becomes dominant. The various phthalocyanines examined have different relative singlet and triplet contributions, for the 8 ns pulse duration used in this study. For SiNc, SiPc and GcPc with $\tau_S \approx 3-5$ ns and $R_T < R_S$, excited-singlet absorption makes a large contribution. On the other hand, for SnPc, with $\tau_S = 2$ ns and $R_T > R_S$, the triplet contribution is more significant and for PbPc, with $\tau_S = 0.7$ ns and $R_T \approx 0.5 R_S$, the triplet contribution is dominant.

4. TRIPLET-TRIPLET ABSORPTION SPECTRA

One consideration in evaluating materials for optical limiting applications is the bandwidth over which the limiting performance is effective. Ideally, for RSA molecules, the ratios R_S and/or R_T would be large over a wide spectral range. The phthalocyanines typically have weak ground state absorption over about a 150 nm range centered at ≈ 500 nm. To determine spectrum of the excited triplet state absorption in group IVA metalloid phthalocyanines, nanosecond transient absorption measurements were conducted. The third harmonic of a Q-switched Nd:YAG at 355 nm with a 10 ns (FWHM) pulse duration was used as an excitation source and a pulsed xenon lamp white-light source was used as a probe. Figure 5 shows the transient difference spectra for SiPc, GcPc and SnPc acquired 100 ns after the excitation. We find that the triplet-triplet absorption spectra of these molecules are essentially independent of the central metal atom and consist of broadband absorption (≈ 120 nm FWHM) with a maximum around 510 nm, well overlapped with the transmission band in the ground-state absorption. These results suggest that the phthalocyanines will exhibit effective broadband optical limiting over the 450-600 nm spectral range for nanosecond or longer pulse durations.

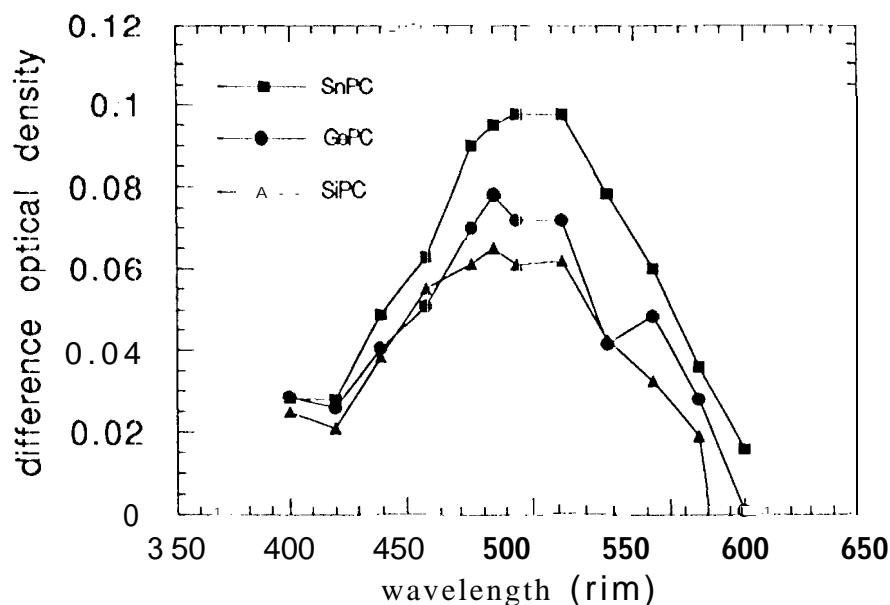


Figure 5 Difference triplet-triplet absorption spectra of SiPc, GcPc and SnPc in toluene.

5. CONCLUSION

It has been demonstrated that the heavy-atom substitution of phthalocyanines leads to enhanced nanosecond nonlinear absorption due to increased population of the strongly absorbing triplet state. A five-state rate-equation model provides a good description of the nonlinear transmission behavior of these dyes for picosecond and nanosecond pulses. The successful simulations of the nonlinear transmission data on this series of phthalocyanines for widely differing pulse durations provide strong evidence for the validity of the excited-state absorption model. Nanosecond transient absorption measurements suggest that the nanosecond optical limiting response of these dyes should span over 150 nm in the visible. PbPc exhibits roughly an order of magnitude lower strong-signal transmission, for picosecond or nanosecond pulses, as compared to CAP. SnPc and PbPc possess large excited-state absorption cross sections and triplet yields, and are quite promising for optical limiting applications.

6. ACKNOWLEDGEMENT

This research was performed at the Jet Propulsion Laboratory (JPL), California Institute of Technology and was supported by the U.S. Army Vulnerability Assessment Laboratory (VAL, LABCOM) through an agreement with the National Aeronautics and Space Administration. D. Alvarez, Jr. thanks the James Irvine Foundation for a postdoctoral fellowship. Support at the Beckman Institute from the Air Force Office of Scientific Research, AASERT Program (Grant #F49620-92-J-0278) is gratefully acknowledged.

7. REFERENCES

1. W. Blau, H. Byrne, W. M. Dennis and J. M. Kelly, *Opt. Commun.*, 56,25-29 (1985),
2. R.C. Hoffman, K.A. Stetyick, R.S. Potember, and D.G. McLean, *J. Opt. Soc. Am. B.*, 6,772-777 (1989).
3. D.R. Coulter, V. M. Miskowski, J.W. Perry, T. H. Wit, E. W. Van Stryland and D. J. Hagan, *Proc. SPIE*, Vol. 110S, 42-51 (1989).
4. L.W. Tutt and S. W. Mc Cahon, *Optics Lett.*, 15,700-702 (1990),
5. J.W. Perry, L.R. Khundkar, D.R. Coulter, D. Alvarez, Jr., S.R. Marder, T.H. Wit, M. J. Sence, E. W. Van Stryland and D.J. Hagan, in *"Organic Molecules for Nonlinear Optics and Photonics,"* J. Messier, F. Kajzar and P. Prasad, Eds. NATO ASI Series E, Vol. 194, pp.369-382 (Kluwer Academic Publishers, Dordrecht, 1991).
6. L. W. Tutt and A. Kost, *Nature*, 356,225 -22,6 (1992),
7. T. H. Wit, D.J. Hagan, M. J. Sence, E. W. Van Stryland, J.W. Perry and D.R. Coulter, *Appl. Phys. B.*, 54, 46-51 (1992),
8. T. Ohno, S. Kate, A. Yamada and T. Tanno, *J. Phys. Chem.*, 87,775 (1983).
9. P. A. Firey, W. E. Ford, J. R. Sounik, M. E. Kenney and M. A. Rodgers, *J. Am. Chem. Soc.*, 110,7626-7630, (1988).
10. J. W. Perry, K. Mansour, E. T. Sleva, K. J. Perry, S. R. Marder and D. Alvarez, Jr., *Conference on Lasers and Electro-Optics*, OSA Technical Digest Series Vol. 12, (Optical Society of America, Washington, DC 1992), pp. 122-123.
11. J.N. Esposito, L.E. Sutton, and M. E. Kenny, *Inorg. Chm.*, 6, 1116-1120 (1967).
12. L. E. Sutton and M. E. Kenny, *Inorg. Chem.*, 6, 1869-1872, (1967).
13. S.A. Mikhalevko, S.V. Barkanova, O.L. Lebedev, E.A. Lukyanov, *Zh. Obshch. Khim. (Engl. Transl.)* 41, 2735 (1971).
14. G. French, U. S. Patent No. 1580683, (1970).
15. P. Sayer, M. Gouterman, and C. R. Connel, *Acc. Chem. Res.*, 15, 73-79 (1982).
16. W. F. Kosonocky and S. E. Harrison, *J. Appl. Phys.*, 37(13), 4789-4797 (1966).
17. R. S. Taylor and S. Mihailov, *Appl. Phys. B*, 38, 131-137 (1985).
18. S. Speiser, *Proc. SPIE*, Vol. 1127, 152-159 (1989).

19. J. W. Wu, J. R. Heflin, R. A. Norwood, K. Y. Wong, O. Zamani-Khamiri, A. F. Garito, P. Kalyanaraman, and J. Sounik, *J. Opt. Soc. Am. B*, 6, 707-720 (1989).
20. G. R. Allan, D. R. Labergerie, S. J. Rychnovsky, T. F. Boggess, A. L. Smirl, and L. Tutt, *J. Phys. Chem*, 96, 6313-6317 (1992).
21. S. J. Strickler and R. A. Berg, *J. Chem. Phys.*, 37, 814 (1962).